The subsolar magnetosheath and magnetopause for high solar wind ram pressure: WIND observations

T. D. Phan[1], D. E. Larson[1], R. P. Lin[1], J. P. McFadden[1], K. A. Anderson[1], C. W. Carlson[1], R. E. Ergun[1], S. M. Ashford[1], M. P. McCarthy[2], G. K. Parks[2], H. Rème[3], J. M. Bosqued[3], C. D'Uston[3], K.-P. Wenzel[4], T. R. Sanderson[4], and A. Szabo[5]

Abstract. On a rapid inward pass through the subsolar magnetosheath (MSH) and magnetopause (MP), the WIND spacecraft initially encountered a moderately-compressed low-magnetic shear MP (at a radial distance of 8.6 R_E), followed by multiple crossings of a high-shear MP (at 8.2 R_E). The large shear resulted from a southward turning of the external MSH field. Strong magnetic field pile-up, a plasma depletion layer (PDL), and plasma flow acceleration and rotation to become more perpendicular to the local magnetic field were observed in the MSH on approach to the low-shear MP. At the high-shear MP, magnetic reconnection flows were detected, and there are some indications that plasma depletion effects were weak or absent in the adjacent MSH. We attribute the changes in the MP and MSH properties to the sudden rotation of the MSH field direction. In essence, the structure of the MP regions under the unusually high solar wind ram pressure condition in this case does not seem to be qualitatively different from that observed under more typical (less compressed) conditions. Also similar to previous observations, the mirror mode is marginally unstable in the MSH proper, but is stable in the PDL. In this region, the proton temperature anisotropy is inversely correlated with $\beta_{p\parallel}$. Finally, the electron distributions are observed to be anisotropic ($T_{e\perp}/T_{e\parallel}$ ~1.3) throughout the entire MSH.

Introduction

The processes responsible for transferring mass, momentum, and energy of solar wind into the magnetosphere are of great interest. Detailed studies of the thin magnetopause (MP), however, are often difficult due to the non-stationary nature of the boundary and also due to the limited resolution of the instruments. Furthermore, information on the global state of the MP cannot be directly deduced from these local observations.

The region of the magnetosheath (MSH) near the MP, on the other hand, is expected to provide information on the state of the large scale MP since the structures of the incoming plasma and magnetic field, in the region extending from the MP to some distance upstream, should be influenced by the physical processes operating in a large area of the MP.

[1]Space Sciences Laboratory, University of California, Berkeley, CA
[2]Geophysics Program, University of Washington, Seattle, WA
[3]Centre d'Etude Spatiale des Rayonnements, Toulouse, France
[4]Space Science Department of ESA, ESTEC, Noordwijk, Netherlands
[5]Laboratory for Extraterrestrial Physics, NASA/GSFC, Greenbelt, MD

On the theoretical side, *Midgley and Davis* [1963], *Lees* [1964], and *Zwan and Wolf* [1976] predicted a decrease of plasma density in the MSH region next to the MP due to the compression of the draped magnetic field lines against the dayside MP. *Zwan and Wolf* also speculated that the depletion process would be less efficient when reconnection occurs at the MP. More recently, motivated by the ISEE observations of a region of enhanced density and reduced magnetic field in the MSH [e.g., *Song et al.*, 1992], *Southwood and Kivelson* [1996] argues that the depletion process proposed by *Zwan and Wolf* requires the presence upstream of a region of slow mode disturbances. In this model, a standing slow mode structure, which lies between the upstream flow region and the PDL, serves to initiate flow deflection away from the subsolar point.

A plasma depletion layer (PDL) is generally observed next to the dayside low shear MP [*Paschmann et al.*, 1993; *Song et al.*, 1993; *Anderson and Fuselier*, 1993; and *Phan et al.*, 1994].

Using data from the AMPTE/IRM spacecraft, which sampled the MSH and the MP under average solar wind conditions, *Phan et al.* [1994] found no evidence of magnetic field pile-up and plasma depletion effects next to high-shear MP. *Phan et al.* interpreted the absence of a PDL as evidence for the violation of the frozen magnetic field condition somewhere at the MP, although signatures of reconnection flows were not always detected at the local MP. The observations of AMPTE/CCE (which had a lower apogee of ~8.8 R_E) of high-shear MSH, on the other hand, indicate the presence of a weak PDL under high external pressure conditions [e.g., *Anderson and Fuselier*, 1993]. One weakness of the CCE evidence however is that the data was sampled at roughly the same radial distance and may not represent a real spatial cut through the subsolar MSH.

In order to discern the effects of solar wind ram pressure on the structures and dynamics of the subsolar MSH and the MP, we examine a rapid crossing by WIND through these regions when the external pressure was unusually high. Furthermore, during this pass the Wind spacecraft encountered both low- and high-shear MPs, which provides an opportunity to observe the effects of the magnetic field rotation on the MP and MSH processes. This is unlike previous work where the influence of the MSH field orientation on the structure of the MSH was deduced by examining a large number of independent passes.

Instrumentation

The present analysis uses data from WIND. Plasma parameters are obtained from the three-dimensional plasma and energetic particle detectors. Proton moments representative of the core MSH and magnetospheric populations are deduced from 3-D distributions measured by a "top-hat" electrostatic analyzer (PESA-H), operating in a mode to detect particles with energies from 80 eV to 27 keV. Although a full 3-D proton distribution is obtained every spacecraft spin period (3s), the distributions are
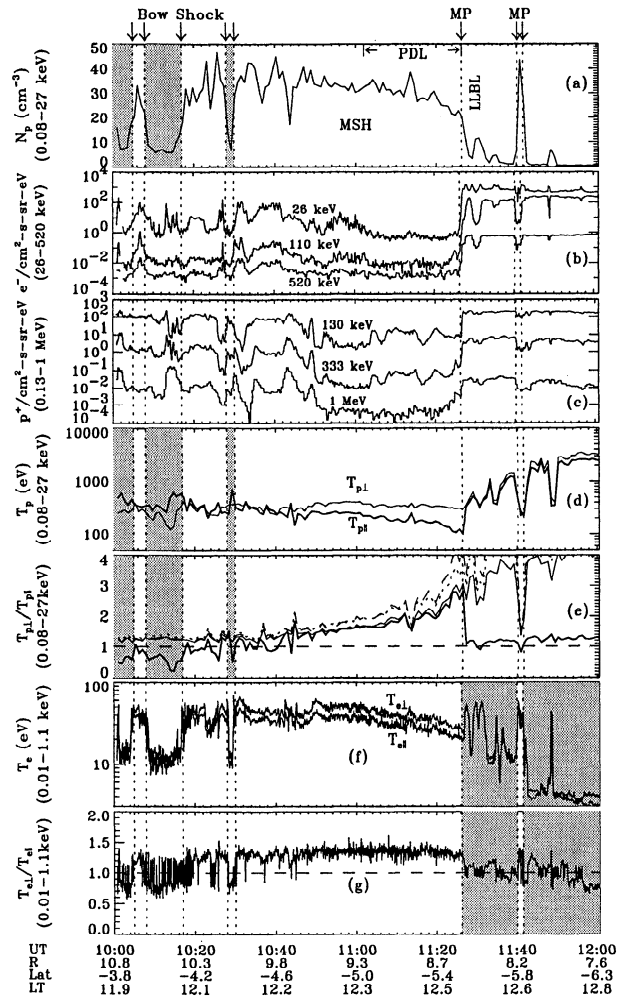
Figure 1. Overview of the inbound pass on December 24, 1994. The figure shows the total proton number density; the energetic electron and proton fluxes; the proton temperatures; and temperature anisotropy (thick solid, solid, dotted, and dashed lines correspond to the measured anisotropy and the predictions from the *Phan et al.*, *Anderson et al.*, and *Fuselier et al.* relations, respectively); the electron temperatures and temperature anisotropy. The shaded areas indicate regions where the plasma moments are not representative of the core population. The crude identification of the PDL is based mainly on the decrease in the plasma temperature and the increase in the proton temperature anisotropy.

Figure 2. The proton bulk speed; the azimuth angle, in the LMN boundary normal coordinate system with 0° along the L axis and +90° along the M axis, and the elevation angle of the flow; the magnetic field strength and angles; the total pressure; the plasma β; and the mirror mode criterion.

averaged on-board for 51s before being transmitted owing to limited telemetry capacity. Note that the transmitted one-spin resolution proton moments obtained from another electrostatic analyzer (PESA-L) are accurate in representing the solar wind population, but not the hotter MSH and magnetospheric core populations and are thus not used in the present study. One-spin resolution electron moments representative of the core MSH population (but not the magnetospheric electrons) are obtained from the on-board moment computation for electrons measured by a electrostatic analyzer (EESA-L) over the energy range of 10 eV to 1.1 keV. Energetic electrons (26 keV - 519 keV) and ions (67 keV - 6.8 MeV) are detected by a pair of semi-conductor detector telescopes, and their distributions are transmitted at rates of one sample every 51 s for protons and one sample every
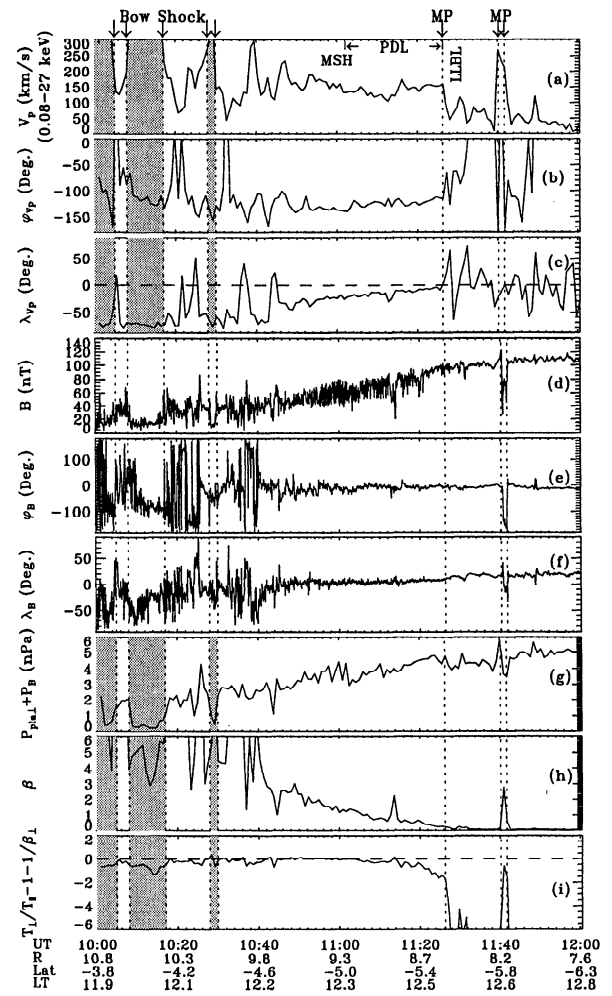
26 s for electrons. The magnetic field is measured at a rate of 10.9 samples/s, but for our analysis the magnetic field data are averaged for 3s. Details of the plasma and magnetic field instruments are described by *Lin et al.* [1995] and *Lepping et al.* [1995].

Observations

Figures 1 and 2 show an overview of the inbound pass from the subsolar bow shock to the magnetosphere on December 24, 1994. At ~1015 UT, the satellite crossed a compressed bow shock and moved into the MSH (the radial distance to the shock was 10.5 R_E). The next half hour witnessed multiple crossings of the bow shock as the MSH was further compressed. The MSH proper was finally reached at ~1044 UT. At 1126 UT (at a radial distance of ~8.6 R_E), the satellite encountered a sharp increase in the proton temperature, T_p (Fig. 1d), together with abrupt changes in the bulk plasma flow speed and direction, φ_{vp} (Fig. 2b), but with almost no changes in the magnetic field direction and magnitude (Fig. 2d-f). These features are signatures of low-shear MPs [*Paschmann et al.*, 1993]. Due to the Earthward

motion of the MP, the satellite made a brief return to the MSH before reaching the magnetosphere proper. The MP was crossed at 1140:30 and 1141:45 UT and is identified most easily by sharp changes in the field direction (Fig. 2e-f). The magnetic shear across the MPs encountered during this excursion is ~150°, indicating that a southward turning of the external MSH magnetic field has occurred after the satellite crossed the first low-shear MP.

We note the following features of the MSH region adjacent to the low-shear MP: (1) the monotonic decrease of the plasma flow angle $|\lambda_{vp}|$ on approach to the MP, indicating that the satellite was steadily traversing a quasi-stationary MSH; (2) the presence of a plasma depletion layer where B increases and N_p and T_p decrease on approach to the MP, accompanied by an increase of the temperature anisotropy $T_{p\perp}/T_{p\parallel}$ (Fig. 1e); (3) the electron temperature (Fig. 1f) also decreases across the depletion region, but the ratio $T_{e\perp}/T_{e\parallel}$ (Fig. 1g) remains close to 1.3 throughout the entire MSH; (4) the marginal stability criterion for the mirror mode, $T_\perp/T_\parallel - [1+ (1/\beta_\perp)] = 0$ [e.g., Hasegawa, 1975], is satisfied throughout the MSH, except in the plasma depletion layer (Fig. 2i); (5) the decrease of the bulk speed, V_p, from the bow shock to the MP, except in the $\beta<1$ region, i.e., in the 10 minute interval preceding the MP crossing, where an enhancement of V_p is observed. This enhancement results from an increase of the component of the flow tangential to the MP (not shown), while the normal component continues to decrease (see the decrease of $|\lambda_{vp}|$). In addition to the flow speed enhancement, the flow also rotates to become more perpendicular to the magnetic field on approach to the MP; the relative angle between the flow and the magnetic field, $|\varphi_B - \varphi_{vp}|$, reduces from ~120° in the MSH proper to ~100° at the MP. Such a flow pattern may be consistent with the formation of a stagnation line, instead of a stagnation point, at the subsolar MP when the MSH magnetic field piles up to a dynamically significant level [e.g., Sonnerup, 1974]; (6) the presence of a region of enhanced density and reduced magnetic field at around 1114 UT. Such density enhancement is somewhat similar to that observed by ISEE [e.g., Song et al., 1992]. However, to establish whether such "structure" is a slow mode wave is beyond the scope of the present paper; (7) the energetic particle fluxes (Fig. 1b-c) are lowest in the MSH region far removed from the bow shock and near the MP, indicating that these particles originate from both the magnetosphere and the bow shock.

At the high-shear MP (at 1140:30 and 1141:45 UT), we note an enhancement of the bulk speed of more than 100 km/s, relative to the low-shear MSH level. Although the low time resolution of the measurements does not permit a detailed study of the MP structure, the flow enhancement is a signature of reconnection. Finally, we note that while the inward motion of the MP which led to the high-shear MP crossings would be consistent with the erosion of the dayside magnetospheric field caused by reconnection initiated when the MSH field turned southward, the more likely cause for the brief encounter with the MSH in this case is a sudden increase in the external pressure at 1140 UT (see Fig. 2g). In addition, the large $|\lambda_B|$ detected at the MP indicates significant undulation of the MP surface.

In the interval between the high-shear MP crossings, i.e., in the MSH, the magnetic field magnitude is greatly reduced relative to the magnetospheric field. Its level is similar to that in the pre-plasma depletion region (at 1145 UT, say). The few ion samples in this region also reveal that the levels of N_p and β, and more importantly the proton temperature anisotropy, are similar to those in the pre-plasma depletion region. These features of the

magnetic field and proton properties strongly suggest that the plasma depletion effects are either weak or absent. An exception to this interpretation would be if an enhancement in the solar wind density and a reduction in the IMF strength accompanied the southward turning of the IMF. Unfortunately, no solar wind or MSH data were available at the times of the high-shear MP crossings to verify our interpretation.

Discussion

We have investigated a WIND pass across the subsolar MSH and MP when the external MSH pressure was unusually high (~4.5 nPa). In addition, a rotation of the MSH magnetic field (presumably caused by a rotation of the IMF) occurred during the multiple crossings of the MP. These unusual circumstances provide an opportunity to discern the effect of the external pressure and of the magnetic field orientation on the state of the MP and on the structure of the adjacent MSH. Below we relate our observations to those made by AMPTE/IRM under more typical (less compressed) solar wind conditions, and also with those sampled by AMPTE/CCE under compressed conditions.

High Magnetic Shear versus Low Magnetic Shear, and the Effects of High Solar Wind Ram Pressure

The presence of a PDL and the acceleration and rotation of the plasma flows on approach to the low-shear MP have been interpreted as evidence for low rate of transfer across the local MP [Phan et al., 1994]. Compared to the MSH profiles observed under more typical solar wind conditions [e.g., Paschmann et al., 1993], a higher external pressure in this case seems to merely enhance the plasma depletion effects: larger proton anisotropy and stronger magnetic field pile-up next to the MP.

Weak or absent of plasma depletion and flux pile up next to the high-shear MP suggests that a fundamental change in the state of the MP had occurred in association with the rotation of the MSH field. The presence of enhanced flows at the high-shear MP (but not at the low-shear MP) is consistent with the reconnection process being responsible for reducing the depletion effects. Note that the effects of the magnetic shear on the MSH processes have also been deduced in previous studies [e.g., Anderson and Fuselier, 1993; Phan et al., 1994] based on the examination of independent passes through the MP.

Temperature Anisotropies and Mirror and Ion-Cyclotron Instabilities in the Magnetosheath

The marginal stability criterion for the mirror mode is satisfied throughout the compressed MSH, except in the PDL. This feature is remarkably similar to the average MSH observed under more typical solar wind conditions [Hill et al., 1995; Phan et al., 1994]. Consistent with these findings, the magnetic field fluctuations are much lower in the PDL than in the MSH proper (Fig. 2d). Note that previous observations of wave properties in highly-compressed MSH also indicate that the PDL is mirror stable [e.g., Anderson et al., 1994]. In this mirror-stable region, Anderson et al. have found the ion-cyclotron waves to be dominant. They also reported an inverse relationship between the proton temperature anisotropy and $\beta_\parallel$ in this region.

The connection between the ion-cyclotron mode and the temperature anisotropy-$\beta_\parallel$ relationship has been extensively investigated theoretically [e.g., Gary et al., 1994]. These studies demonstrated that wave particle scattering by ion cyclotron anisotropy instability produces a correlation of the form

$T_{p\perp}/T_{p\parallel} = 1 + c\beta_{p\parallel}{}^b$, where b is around -0.5 and c varies between 0.5 and 1. The value of c depends on a number of factors, including the Helium concentration [e.g., *Gary et al.*, 1994].

Using CCE data, *Anderson et al.* [1994] and *Fuselier et al.* [1994] found the relations $T_{p\perp}/T_{p\parallel} = 1 + 0.85\beta_{p\parallel}{}^{-0.48}$ and $T_{p\perp}/T_{p\parallel} = 1 + 0.83\beta_{p\parallel}{}^{-0.58}$ to hold in the MSH downstream of quasi-perpendicular and quasi-parallel shocks, respectively. The IRM observations of the average MSH next to low-shear MPs, on the other hand, satisfy $T_{p\perp}/T_{p\parallel} = 1 + 0.63\beta_{p\parallel}{}^{-0.50}$ [*Phan et al.*, 1994]. For the present event, we found the relation $T_{p\perp}/T_{p\parallel} = 1 + 0.56\beta_{p\parallel}{}^{-0.49}$ to hold in the PDL, i.e., in the 1100-1125 UT interval. Figure 1e shows $T_{p\perp}/T_{p\parallel}$ as predicted by the CCE and IRM relations, based on the measured $\beta_{p\parallel}$, together with the WIND measured anisotropy. It is noted that the anisotropy in the MSH measured by WIND (thick solid line) agrees remarkably well with the IRM relation (solid line) in the PDL. All these observations, which found the temperature anisotropy to be inversely correlated with $\beta_{p\parallel}$, with an exponent ~ -0.5, are consistent with the ion-cyclotron mode playing a major role in the evolution of the plasma in the PDL. The variation in the coefficients found in the various studies is not fully understood. It may be due to the factors examined by *Gary et al.* [1994].

Finally, we note that since the mirror-mode criterion involves quantities from both the magnetic field and the plasma measurements, our observation of the well-known fact that the mirror mode marginal stability criterion is satisfied in the MSH proper indicates that these quantities are fairly well measured.

As shown in Figure 1g, the thermal electron temperature anisotropy, $T_{e\perp}/T_{e\parallel}$, is below unity in the solar wind, but becomes greater than one across the bow shock. But unlike $T_{p\perp}/T_{p\parallel}$ which increases with decreasing β on approach to the low-shear MP, $T_{e\perp}/T_{e\parallel}$ remains rather constant at ~1.3 throughout the entire MSH. This is in contrast with the IRM observations of nearly isotropic electron distributions in the MSH [e.g. *Paschmann et al.*, 1993]. The difference between the Wind and IRM findings is presently not understood.

It should be pointed out that anisotropic distributions have been reported in the MSH for suprathermal (1-20 keV) electrons [*Gosling et al.*, 1989]. However, *Gosling et al.* found that the anisotropy did not originate at the bow shock, but rather, it developed in the MSH. The source of anisotropy in the thermal electron distributions remains unclear, but our observations suggest that it is generated at or near the bow shock.

In conclusion, comparisons of our observations with those sampled under more typical solar wind conditions [*Paschmann et al.*, 1993; *Phan et al.*, 1994] indicate that doubling the total pressure of the MSH (from 2 nPa for average conditions to 4.5 nPa for this event) has not affected the large-scale structure of the MSH and MP significantly. Our findings also imply that the microphysics in the MSH has not been modified by the additional compression of the MSH. It remains to be seen when and how even stronger compression could change the properties of these regions.

References

Anderson, B. J., and S. A. Fuselier, Magnetic pulsations from 0.1 to 4.0 Hz and associated plasma properties in the Earth's subsolar magnetosheath and plasma depletion layer, *J. Geophys. Res.*, *98*, 1461-1479, 1993.

Anderson, B. J., et al., Magnetic spectral signatures in the Earth's magnetosheath and plasma depletion layer, *J. Geophys. Res.*, *99*, 5877-5891, 1994.

Fuselier, S. A., et al., Inverse correlations between the ion temperature anisotropy and plasma beta in the Earth's quasi-parallel magnetosheath, *J. Geophys. Res.*, *99*, 14931-14936, 1994.

Gary, S. P., et al., The proton cyclotron instability and the anisotropy / β inverse correlation, *J. Geophys. Res.*, *99*, 5903-5914, 1994.

Gosling, J. T., et al., Suprathermal electrons at Earth's bow shock, *J. Geophys. Res.*, *94*, 10011-10025, 1989.

Hasegawa, A., *Plasma Instabilities and Nonlinear Effects*, p. 95, Springer, New York, 1975.

Hill, P., et al., and H. Lühr, Plasma and magnetic field behavior across the magnetosheath near local noon, *J. Geophys. Res.*, *100*, 9575-9583, 1995.

Lees, L., Interaction between the solar wind plasma and the geomagnetic cavity, *AIAA J.*, *2*, 1576-1582, 1964.

Lepping, R. P., et al., The Wind magnetic field investigation, *Space Science Review*, *71*, 207-229, 1995.

Lin, R. P., et al., A three-dimensional plasma and energetic particle investigation for the Wind spacecraft, *Space Science Review*, *71*, 125-153, 1995.

Midgley, J. E., and L. Davis, Calculation by a moment technique of the perturbation of the geomagnetic field by the solar wind, *J. Geophys. Res.*, *68*, 5111-5123, 1963.

Paschmann, G., et al., Structure of the dayside magnetopause for low magnetic shear, *J. Geophys. Res.*, *98*, 13,409-13,422, 1993.

Phan, T.-D., et al., The magnetosheath region adjacent to the dayside magnetopause: AMPTE/IRM observations, *J. Geophys. Res.*, *99*, 121-141, 1994.

Song, P., et al., Slow mode transition in the frontside magnetosheath, *J. Geophys. Res.*, *97*, 8295, 1992.

Song, P., et al., Structure and properties of the subsolar magnetopause for northward IMF: multiple-instrument observations, *J. Geophys. Res.*, *98*, 11,319-11,337, 1993.

Sonnerup, B. U. Ö., The reconnecting magnetosphere, in *Magnetosphere Physics*, B. M. McCormac, ed., pp. 23-33, D. Reidel Publ. Co. Dordrecht Holland, 1974.

Southwood, D. J., and M. G. Kivelson, Magnetosheath flow near the subsolar magnetopause: Zwan-Wolf and Southwood-Kivelson theories reconciled, *J. Geophys. Res.*, in press, 1996.

Zwan, B. J., and R. A. Wolf, Depletion of solar wind plasma near a planetary boundary, *J. Geophys. Res.*, *81*, 1636-1648, 1976.

T. D. Phan, D. E. Larson, R. P. Lin, J. P. McFadden, K. A. Anderson, C. W. Carlson, R. E. Ergun, and S. M. Ashford, Space Sciences Laboratory, University of California, Berkeley, CA 94720-7450. (email: phan@ssl.berkeley.edu)

M. P. McCarthy and G. K. Parks, Geophysics, Box 351650, University of Washington, Seattle, WA 98195-1650

H. Rème, J. M. Bosqued, and C. D'Uston, Centre d'Etude Spatiale des Rayonnements, B.P. 4346, 31029 Toulouse Cedex, France

K.-P. Wenzel and T. R. Sanderson, Space Science Department of ESA, ESTEC, Domeinweg, 2200 AG Noordwijk, Netherlands

A. Szabo, Laboratory for Extraterrestrial Physics, NASA/GSFC, Greenbelt, MD 20771